CRITERION-III

RESEARCH, INNOVATIONS AND EXTENSION

3.3 RESEARCH PUBLICATIONS AND AWARDS

3.3.1 Number of research papers published per teacher in the Journals notified on UGC CARE list

Link to website of the Journal

Index

Research papers published in 2018

Sr. No.	Title of paper	Name of the author/s	Department of the teacher	Name of Journal ISSN number	Link to article / paper / abstract of the article
1	Magnetic Nanoparticle Decorated NHeterocyclic Carbene–Nickel Complex with Pendant Ferrocenyl Group for C–H Arylation of Benzoxazole	Altafhusen Naikwade, Megha Jagadale, Dolly Kale, Shivanand Gajare, Prakash Bansode, Gajanan Rashinkar	Chemistry	Catalysis Letters 1572-879X	https://link.springer.com/article/10.1007/s10562-018-2514-1
2	DNA barcode based delineation of freshwater fishes from northern Western Ghats of India, one of the world's biodiversity hotspots	Patil, T. S., Jamdade, R. A., Patil, S. M., Govindwar, S. P., & Muley, D. V.	Zoology	Biodiversity and Conservation 1572-9710	https://doi.org/10.1007/s10531-018-1604-0
3	Interior ideals in Gsemirings	R.D. Jagatap	Mathematics	Malaya Journal of Matematik 2319-3786	https://www.malayajournal.org/archive/selected_article.php?id=501
4	Geochemical Evidences for Possible Absence of CuSulfide Deposits in the Deccan Volcanic Province, India.	Laxman, M. B., & Kumar , K. V .	Geology	Journal Of The Geological Society Of India 0016-7622	https://link.springer.com/article/10.1007/s12594-018-1033-4
5	Copper ferrite magnetic nanoparticles for the immobilization of enzyme	S. V. Otari, S. K. S. Patel, S-Y. Kim, J. R. Haw, V. C. Kalia, I-W. Kim, J-K. Lee	Microbiology	Indian Journal of Microbiology 0973-7716	https://link.springer.com/article/10.1007/s12088-018-0768-3

Co-ordinator,
Internal Quality Assurance Cell (IQAC),
Yashwantrao Chavan College of Science, Karad

Principal,
Yashwantrao Chavan College of Science, Karad

6	SiO2 microparticles with carbon nanotube- derived mesopores as an efficient support for enzyme immobilization	A. Kumar, G. D. Park, S. K. S. Patel, S. Kondaveeti, S. V. Otari, M. Z. Anwar, V. C. Kalia, S. C. Kim, B-K. Cho, J-H. Sohn, D-R. Kim, J-K. Lee, Y. C. Kang	Microbiology	Chemical Engineering Journal 1385-8947	https://www.sciencedirect.com/science/article/abs/pii/S1385894718322861
7	Geochemistry of upland laterites of Tarale –Thoseghar Plaeau of Bamnoli range of Satara district of Maharshtra	Desai R.V., Khanapurkar J.V. and Suryawanshi R. A.	Geology	Journal of Applied Geochemistry 2319-4316	https://www.indianjournals.com/ijor.aspx?target=ijor:jag&volume=20&issue=4&article=004
8	Petrographical and mineralogical studies on lateritic bauxite profiles of Shahuwadi taluka of Kolhapur district, Maharashtra	Khanpurkar J.V., Suryawanshi R.A., Desai R.V., Patil S.H., Mali V. R. and Pisal P.B.	Geology	Journal of Applied Geochemistry 2319-4316	https://www.indianjournals.com/ijor.aspx?target=ijor:jag&volume=20&issue=4&article=005
9	Emplacement and growth of alkaline dikes: Insights from the shonkinite dikes (Elchuru alkaline complex, SE India).	Ghodke, S. S., Rathna, K., Kokandakar , G. J., Nagaraju, B., More, L. B., Bhosle, M. V ., & Kumar , K. V	Geology	Journal Of Structural Geology 0191-8141	https://doi.org/10.1016/j.jsg.2018.09.016

Co-ordinator,
Internal Quality Assurance Cell (IQAC),
Yashwantrao Chavan College of Science, Karad

Principal,
Yashwantrao Chavan College of Scien
Karad

Catalysis Letters (2018) 148:3178–3192
https://doi.org/10.1007/s10562-018-2514-1

Magnetic Nanoparticle Decorated *N*-Heterocyclic Carbene–Nickel Complex with Pendant Ferrocenyl Group for C–H Arylation of Benzoxazole

Altafhusen Naikwade[1] · Megha Jagadale[1] · Dolly Kale[1] · Shivanand Gajare[1] · Gajanan Rashinkar[1]

Received: 7 May 2018 / Accepted: 29 July 2018 / Published online: 16 August 2018

Abstract

Magnetic nanoparticle decorated *N*-heterocyclic carbene–nickel complex with pendant ferrocenyl group has been prepared by multi-step procedure. The formation of complex was confirmed on the basis of analytical techniques such as Fourier transform infrared (FT-IR), Fourier transform Raman (FT-Raman) and X-ray photoelectron spectroscopy (XPS) as well as by X-ray diffraction (XRD), transmission electron microscopy (TEM) and vibrating sample magnetometer (VSM) analysis. The complex proved to be an efficient heterogeneous catalyst for C–H arylation of benzoxazole with aryl boronic acids. The recycling studies revealed that complex could be reused for six times without significant decrease in catalytic activity.

Graphical Abstract

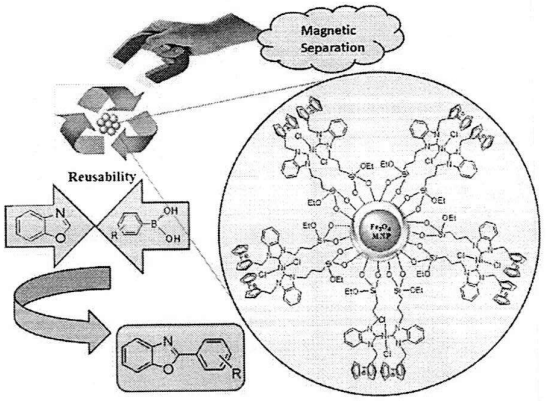

Keywords *N*-Heterocyclic carbenes · Fe_3O_4 nanoparticles · Ferrocene · C–H arylation · Reusability

1 Introduction

N-Heterocyclic carbenes (NHCs) represent most significant class of ligands with wide spread and spectacular applications [1–6]. The choice of NHCs as best ligands can be rationalized by their incomplete electron octet, coordinative unsaturation strong σ-donor capacity, comparatively weak π-acceptor property and sterically demanding structure [7–14]. In addition, due to modular design of NHCs

Electronic supplementary material The online version of this article (https://doi.org/10.1007/s10562-018-2514-1) contains supplementary material, which is available to authorized users.

✉ Gajanan Rashinkar
gsr_chem@unishivaji.ac.in

[1] Department of Chemistry, Shivaji University, Kolhapur, Maharashtra 416004, India

Biodiversity and Conservation
https://doi.org/10.1007/s10531-018-1604-0

ORIGINAL PAPER

DNA barcode based delineation of freshwater fishes from northern Western Ghats of India, one of the world's biodiversity hotspots

Tejas S. Patil[1] · Rahul A. Jamdade[2] · Swapnil M. Patil[3] · Sanjay P. Govindwar[4] · Dipak V. Muley[1]

Received: 16 June 2017 / Revised: 27 July 2018 / Accepted: 9 August 2018

Abstract

DNA barcodes analyzed by using relevant techniques provide an imperative approach towards validation of prevailing taxa and putative species. Here, molecular methods were used for assessment of 246 barcodes belonging to 81 fish species from northern Western Ghats of India, using, Barcode gap analysis, barcode index number, automatic barcode gap discovery, Poisson tree processes and general mixed Yule-coalescent, these methods had their potential to discriminate 97.53%, 93.90% 95.06%, 93.82% and 92.59% of species respectively. But, some of them tended to estimate the inconsistent number of species leading to discrepancies between the morphological concept and inference from molecular phylogenetic reconstructions. So, we took a standard approach to recognize those methods that produced consistent results, three of five such methods were identified that revealed three hidden cryptic species complexes in *Monopterus indicus*, *Parambassis ranga* and *Systomus sarana*. Further, to validate these three genetically diverged species, we used diagnostic character based approach along with nine unidentified species through BLOG and WEKAs SMO classifier. Those methods were unable to identify these species, which might be due to the limited number of specimens used for the analysis. This is the first effort to generate the DNA barcode reference library of freshwater fishes from northern Western Ghats of India, one of the world's biodiversity hotspots. These barcodes when analyzed through the defined workflow, will provide valuable measures to prove the efficiency of molecular species delimitation methods in taxonomic discrimination which aid conservation of biodiversity.

Keywords DNA barcoding · Fish diversity · Species delineation · Western Ghats

Communicated by Mark James Kennard.

Electronic supplementary material The online version of this article (https://doi.org/10.1007/s10531-018-1604-0) contains supplementary material, which is available to authorized users.

✉ Dipak V. Muley
drdvmuley@gmail.com

Extended author information available on the last page of the article

Published online: 21 August 2018

Malaya Journal of Matematik, Vol. 6, No. 4, 731-735, 2018

https://doi.org/10.26637/MJM0604/0005

Interior ideals in Γ-semirings

R.D. Jagatap[1*]

Abstract

The concepts of an interior ideal, minimal interior ideal and an interior-simple Γ-semiring are defined. Various properties of an interior ideal and minimal interior ideal of a Γ-semiring are studied. Some characterizations of a minimal interior ideal and an interior-simple Γ-semiring are discussed.

Keywords

Interior ideal, minimal interior ideal , interior-simple Γ-semiring, regular Γ-semiring, intra-regular Γ-semiring.

AMS Subject Classification

16Y60, 16Y99.

[1] *Department of Mathematics, Y.C.College of Science, Karad-415124, Maharashtra, India.*

***Corresponding author**: jagatapravindra@gmail.com

Article History: Received **24** July **2018**; Accepted **17** September **2018**

Contents

1. Introduction

Γ-semiring is a generalization of a semiring. Rao [7] defined and studied Γ-semiring. Dutta and Sardar [1] studied different types of ideals in a Γ-semiring. Quasi-ideals and bi-ideals in a Γ-semiring were studied by Author [2–4]. Lajos [6] defined the concept of an interior ideal in a semigroup. Interior ideal in a semigroup was studied by Szasz [8, 9]. Interior ideals in ordered semigroups and the interior ideal elements in poe-semigroups were discussed by Kehayopulu [5].

The concepts of an interior ideal and minimal interior ideal in a Γ-semiring are introduced in this paper. Some properties of an interior ideal and minimal interior ideal of a Γ-semiring are proved. Some characterizations of a minimal interior ideal are studied. Also the notion of an interior-simple Γ-semiring is defined. Some properties and characterizations of an interior-simple Γ-semiring are furnished. For the concepts in a Γ-semiring see Dutta and Sardar [1] and Jagatap and Pawar [2, 4].

Now onwards S denotes a Γ-semiring with absorbing zero unless otherwise stated.

2. Interior Ideals

Here we define the notion of an interior ideal of a Γ-semiring S.

Definition 2.1. *A non-empty subset I of a Γ-semiring S is an interior ideal of S if I is an additive subsemigroup of S and $S\Gamma I\Gamma S \subseteq I$.*

Example : Let $S = \{0,1,2,3,4\}$. Define two binary operations + and $\cdot$ on S as follows:

+	0	1	2	3	4
0	0	1	2	3	4
1	1	2	3	4	2
2	2	3	4	2	3
3	3	4	2	3	4
4	4	3	2	4	2

.	0	1	2	3	4
0	0	0	0	0	0
1	0	1	2	3	4
2	0	2	4	3	2
3	0	3	3	3	3
4	0	4	2	3	4

For $\Gamma = S$, both S and Γ are additive commutative semigroups. A mapping $S \times \Gamma \times S \to S$ is defined as $a\alpha b =$ usual product of a, α, b; for all $a, b \in S$ and $\alpha \in \Gamma$. Then S forms a Γ-semiring. $\{0\}$, $\{0,3\}$, $\{0,2,3,4\}$ and S are interior ideals of S.

Remark 2.2. *Every ideal is an interior ideal of S but not conversely.*

JOURNAL GEOLOGICAL SOCIETY OF INDIA
Vol.92, October 2018, pp.393-403

Geochemical Evidences for Possible Absence of Cu-Sulfide Deposits in the Deccan Volcanic Province, India

More B. Laxman and K. Vijaya Kumar*
School of Earth Sciences, SRTM University, Nanded - 431606, India
*E mail:vijay_kumar92@hotmail.com

ABSTRACT

Continental flood basalt provinces (CFBs) are important hosts for large-scale Cu-sulfide deposits. However, sulfide mineralization is yet to be discovered, if any, in the end-Cretaceous Deccan volcanic province, India. In the present study, geochemical evidences for the possible absence of Cu-sulfide deposits associated with the Deccan basalts by analyzing and comparing the geochemistries of the Deccan and Siberian CFBs are provided. The Fe-rich nature and high fO_2 conditions did not favour sulfide saturation at any stage of magma evolution in the Deccan province. Crustal contamination of the Deccan magmas also did not increase the sulfur budget. The most contaminated basalts of Bushe and Poladpur formations of the Deccan province do not show any depletion in the copper contents compared to other formations. In the absence of sulfide saturation, copper behaved as an incompatible element in the Deccan magmas in contrast to the Siberian basalts, in which copper behaved as a compatible element during magma evolution due to sulfide saturation consequently formed world-class copper sulfide deposits. It is demonstrated that the lithosphere- and asthenosphere-derived Deccan magmas have similar Cu abundances thereby suggesting that the Cu-sulfide deposits associated with the CFBs are process-controlled rather than source-controlled. Although Cu-sulfide deposits may not have formed, the geochemical patterns suggest favourable conditions for native copper mineralization in the Deccan volcanic province. In the present study, a set of geochemical proxies that can be utilized as preliminary exploration tools for Cu-sulfide mineralization in the CFBs is proposed.

INTRODUCTION

Copper sulfide ore formation in continental flood basalts (CFBs) is a much-debated topic in the realm of magmatic ore deposits. Some of the CFBs designated as "fertile provinces" are hosts to large-scale Cu, Ni and PGE sulfide deposits (for example Siberia, Emeishan, Tarim, Karoo provinces; Zhang et al., 2008); however, some other CFBs designated as "barren provinces" are devoid of sulfide deposits (for example Deccan, Parana, Ferrar provinces; Zhang et al., 2008). Zhang et al. (2008) and Griffin et al. (2013) argued that the ancient cratonic lithospheres contributed substantially to the budget of Cu and Ni to the plume magmas, which eventually formed large sulfide deposits associated with the fertile CFBs; whereas in the barren CFBs, sub-continental lithosphere contribution was minimal. Alternately, Lee et al. (2012) suggested that copper abundances are not distinctly different in the plume-, arc- and ridge-derived primary basaltic magmas consequently inferred that the ore deposit formation is linked to magma evolution process rather than mantle source and primary melt compositions.

In either case (*source-controlled* or *process-controlled*), ultimate formation of the sulfide deposit requires concentration of the ore and its separation from the silicate fraction. Factors that influence sulfur-saturation of the magma and physical segregation of sulfide minerals include (1) degree of mantle melting, (2) FeO, SiO_2 and Na_2O+K_2O contents in the magma, (3) fO_2 and fS_2 fugacities, (4) P-T conditions, (5) assimilation of crustal sulfur and (6) liquid immiscibility. Moderate degrees of mantle melting (~ 20%) produce highest amount of sulfur in the melt (Keays, 1995; Arndt et al., 2005). At lower degrees of melting sulfide phase would be in mantle residue and higher degrees of melting results in the dilution of sulfur in the melt (Wendlandt, 1982; Keays, 1995; Rehkämper et al., 1999). Lower concentration of FeO, high concentrations of SiO_2, $Na_2O + K_2O$ are favourable for sulfide ore formation (MacLean, 1969; Haughton and Roeder, 1974; Buchanan and Nolan, 1979; Naldrett, 2004). Sulfur content needed for sulfide saturation increases exponentially with fO_2 (Jugo et al., 2005; Jugo, 2009). It was estimated that 1300 ppm S is sufficient to induce sulfide saturation at FMQ-1 and 1500 ppm at FMQ+1 for MORB; 7500 ppm at FMQ+2 for back-arc and ocean island basalts and can be as high as 1.4 wt.% at FMQ+2.3 for island-arc basalts (Jugo, 2009). At FMQ+2 conditions, most of the sulfur occurs in sulfate state which has 10 times higher solubility than sulfide (Carroll and Rutherford, 1987; Jugo et al., 2005; Mungall et al., 2006; Jugo, 2009). High temperature magmas dissolve higher amounts of sulfur (Naldrett, 2004; Barnes and Lightfoot, 2005) whereas decreasing pressure increases S solubility in the magma (Mavrogenes and O'Neil, 1999). Therefore, rapid adiabatic ascent of the magma would shift the magmas into the field of sulfur undersaturation (Mavrogenes and O'Neill, 1999) thereby inhibits sulfide ore formation. Crustal contamination is a key process which brings S-undersaturated tholeiitic basaltic magmas to S-saturation and subsequent sulfide ore formation (Brugmann et al., 1993; Wooden et al., 1993; Lightfoot et al., 1990, 1993 and 1994; Hawkesworth et al., 1995; Naldrett et al., 1992, 1995; Lightfoot and Keays, 2005). Assimilation of crustal material is a crucial factor in sulfide saturation because it will influence temperature, SiO_2, Na_2O+K_2O and also adds sulfur to the magma. Solubility of sulfide in mafic-ultramafic magmas decreases with increasing $aSiO_2$ and aNa_2O (MacLean, 1969). Addition of sulfur from the crustal sources to the mantle-derived magmas aids to raise sulfur saturation to the levels at which sulfide segregates (Naldrett, 1999; Naldrett et al., 1992; Lesher and Campbell, 1993; Ripley et al., 2002; Arndt et al., 2005; Lightfoot and Keays, 2005; Wilson and Churnett, 2006). The relationship between assimilation of crustal sulfur by parental magmas and segregation of magmatic sulfides is well recognized in Noril'sk-Talnakh, Voisey's bay and Tarim Basin (Naldrett, 1999).

One geochemical feature that is firmly established in the CFBs is chalcophile element (Cu, Ni, PGE) depletion in silicate magmas (basalts) associated with sulfide ores (Brugmann et al., 1993; Czamankse et al., 1994; Fedorenko, 1994; Lightfoot et al., 1994; Lightfoot and Keays, 2005). The erupted basalts, equilibrated with sulfide ore, are supposed to show chalcophile depletion whether sulfide saturation took place in large deep magma chambers (Brugmann et al., 1993), in narrow shallow magma chambers (Rad'ko, 1991; Naldrett

0016-7622/2018-92-4-393/$ 1.00 © GEOL. SOC. INDIA | DOI: 10.1007/s12594-018-1033-4

Indian J Microbiol (Jan–Mar 2019) 59(1):105–108
https://doi.org/10.1007/s12088-018-0768-3

SHORT COMMUNICATIONS

Copper Ferrite Magnetic Nanoparticles for the Immobilization of Enzyme

Sachin V. Otari[1] · Sanjay K. S. Patel[1] · Sang-Yong Kim[2] · Jung Rim Haw[1] · Vipin C. Kalia[1] · In-Won Kim[1] · Jung-Kul Lee[1]

Received: 23 October 2018 / Accepted: 12 November 2018 / Published online: 30 November 2018

Abstract In this study, novel, hollow superparamagnetic copper ferrite ($CuFe_2O_4$) nanoparticles (NPs) were synthesized by a low-temperature hydrothermal method. The hollow magnetic spheres were characterized by field emission scanning electron microscopy and high resolution transmission electron microscopy to confirm their morphology and size. The hollow NPs were demonstrated as the support for biological materials by the immobilization of *Thermomyces lanuginosus* lipase on the inner and outer surfaces of the hollow spheres. The immobilization of the enzyme was confirmed by Fourier Transform Infra-red spectroscopy and confocal laser scanning microscopy. The immobilized enzyme was shown to have an immobilization efficiency of 84.5%, with approximately 176 mg g^{-1} of enzyme loading, for the hollow-NPs support. The immobilized enzyme exhibited high storage and temperature stability. The reusability of the immobilized lipase was more than 80% after 10 cycles of repeated use.

Keywords Immobilization · Hollow nanosphere · Lipase · Magnetic nanoparticles · Storage stability

Thermomyces lanuginosus lipase is an industrially important enzyme catalyzing various reactions including esterification, hydrolysis, and polymerization, among others. Therefore, lipase has been used in the industrial manufacture of various products such as food, biodiesel, detergent, pharmaceuticals, leather, textiles, and cosmetics [1]. Due to its high cost, low stability in some environmental conditions, and its non-reusability, large-scale application of lipase in industry is rare. In the present study, we achieved the immobilization of this biocatalyst on a suitable support, which could provide a solution for the above-mentioned problems by facilitating reusability and sustainable stability and thus making the process economic. Various methods (via covalent bonding, adsorption, ionic interactions, etc.) and supports (organic and inorganic) have been reported for the immobilization of enzymes [2–6]. Among the different supports, functionalized magnetic NPs have been considered as an ideal support for lipase carrier, enabling easy separation by external magnetic field. Various structured magnetic NPs for lipase have been demonstrated, for a vast variety of applications, and with long-term stability [7–9]. Akyl et al. [10] used dense spherical magnetic Fe_3O_4 NPs for the immobilization of lipase during the synthesis of different forms of lipids. The chitosan functionalized Fe_3O_4 NPs were used for the immobilization of *Thermomyces lanuginosus* lipase for ascorbyl palmitate synthesis [11]. Liu et al. demonstrated use of hollow Fe_3O_4 NPs for lipase support for high stability at 60 °C [12]. Here, hydrothermally synthesized $CuFe_2O_4$ hollow NPs are presented as an effective and efficient support for lipase immobilization. $Cu(NO_3)_2$ and $Fe(NO_3)_3$ were dissolved in glycerol and propanol in a 50-mL Teflon-lined hydrothermal reactor and heated at 180 °C for 22 h to form hollow $CuFe_2O_4$ NPs after calcination at 600 °C for 2 h. The field emission scanning electron microscopy (FE-SEM) images revealed that the as-prepared magnetic NPs are hollow and spherical in structure, with plate-like rough surfaces that acted as sites

✉ In-Won Kim
inwon@konkuk.ac.kr

✉ Jung-Kul Lee
jkrhee@konkuk.ac.kr

[1] Division of Chemical Engineering, Konkuk University, Seoul 05029, Republic of Korea

[2] Department of Food Science and Biotechnology, Shin-Ansan University, Ansan 15435, Republic of Korea

Chemical Engineering Journal 359 (2019) 1252–1264

Contents lists available at ScienceDirect

Chemical Engineering Journal

journal homepage: www.elsevier.com/locate/cej

SiO_2 microparticles with carbon nanotube-derived mesopores as an efficient support for enzyme immobilization

Ashok Kumar[a,1], Gi Dae Park[b,1], Sanjay K.S. Patel[a,1], Sanath Kondaveeti[a], Sachin Otari[a], Muhammad Zahid Anwar[a], Vipin C. Kalia[a], Yogendra Singh[a], Sun Chang Kim[c,d], Byung-Kwan Cho[c,d], Jung-Hoon Sohn[e], Dong Rip Kim[f], Yun Chan Kang[b,*], Jung-Kul Lee[a,*]

[a] Department of Chemical Engineering, Konkuk University, 1 Hwayang-Dong, Gwangjin-Gu, Seoul 05029, Republic of Korea
[b] Department of Materials Science and Engineering, Korea University, Anam-Dong, Seongbuk-Gu, Seoul 02841, Republic of Korea
[c] Department of Biological Sciences and KI for the BioCentury, Korea Advanced Institute of Science and Technology, Daejeon 34141, Republic of Korea
[d] Intelligent Synthetic Biology Center, Daejeon 34141, Republic of Korea
[e] Cell Factory Research Center, Korea Research Institute of Bioscience & Biotechnology (KRIBB), Daejeon 34141, Republic of Korea
[f] School of Mechanical Engineering, Hanyang University, Seoul 04763, Republic of Korea

HIGHLIGHTS

- Mesoporous SiO_2 is synthesized by spray pyrolysis using carbon nanotubes as a template.
- Mesoporous SiO_2 microparticles have been successfully used to immobilize enzyme.
- Mesoporous SiO_2 provides an excellent support for enzyme in biosensor or biocatalysis.

GRAPHICAL ABSTRACT

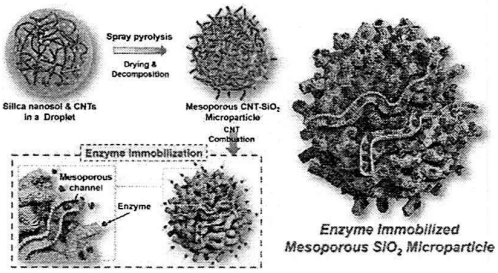

ARTICLE INFO

Keywords:
Mesoporous silica
Enzyme immobilization
Hydrophobicity
Biosensor
Stability

ABSTRACT

Novel mesoporous SiO_2 microparticles were synthesized by spray pyrolysis using multiwalled carbon nanotubes (MCNTs) as a template. The synthesized multicompartment structure with uniform pores of 12.0 nm was used to immobilize lipase from *Thermomyces lanuginosus*. The total surface area of mesoporous SiO_2 microparticles prepared from silica colloidal solution was increased by 26-folds compared to that of dense SiO_2 particles (494 vs 19.0 $m^2 g^{-1}$, respectively). Mesoporous SiO_2 particles showed 236% higher protein loading for lipase, than dense SiO_2 particles. The maximum velocity (V_{max}) and catalytic efficiencies of immobilized lipase were 3.80 and 5.90 folds higher than that of free enzyme. Contact angle analysis revealed increased hydrophobicity of the mesoporous particles, which is advantageous for lid opening at the active center, and increased activity after immobilization. We next developed a lipase/SiO_2/glassy carbon electrode (GCE) biosensors. Cyclic voltammetric results showed linear responses of the lipase/SiO_2/GCE bioelectrode towards tributyrin (50–300 mg dL^{-1}) as a surface-limited reaction in Tris-HCl buffer. After 12 repetitive uses, dense SiO_2- and mesoporous SiO_2-bound lipase retained 74.2 and 95.4% of its original activities, respectively. Thus, given their desirable characteristics and industrial utility, greatly porous SiO_2 particles may provide an excellent support for enzyme immobilization in biosensor development or biocatalysis in organic media.

* Corresponding authors.
E-mail addresses: yckang@korea.ac.kr (Y.C. Kang), jkrhee@konkuk.ac.kr (J.-K. Lee).
[1] These authors contributed equally to this work.

https://doi.org/10.1016/j.cej.2018.11.052
Received 13 August 2018; Received in revised form 13 October 2018; Accepted 7 November 2018
Available online 10 November 2018
1385-8947/

Journal of Applied Geochemistry
Vol. 20, No. 4 (2018). pp. 421-431

GEOCHEMISTRY OF UPLAND LATERITES OF TARALE - THOSEGHAR PLATEAU OF BAMNOLI RANGE OF SATARA DISTRICT OF MAHARASHTRA, INDIA

R.V. Desai*[1], J.V. Khanapurkar[2], R.A. Suryawanshi[1]
[1]*Department of Geology, Yashwantrao Chavan College of Science, Karad*
[2]*Department of Geology, Gopal Krishna Gokhale College, Kolhapur*
**Email id- rajeshdesai27geology@gmail.com*

Abstract

Bamnoli range covers the western part of Satara and Patan taluk of Satara districts and mainly consist of hard lateritic plateaus with an altitude of more than 1000 m. Laterites of in study area are formed due to intense chemical weathering of the parent basalt. The transformation of basalt to laterite is traced by studying major and trace elements from different horizons and their inter-relation plots exhibit differential mobility of elements. X-ray diffraction and Infrared Spectroscopy of the plateau laterite and lithomarge clay samples indicate the presence of hematite, goethite, maghemite, kaolinite, gibbsite, quartz, ilmenite and rarely montmorillonite, metahalloysite. Wt % of Fe_2O_3, Al_2O_3 and SiO_2 in the laterites of the study area ranges between 35.61- 51.69, 13.23- 22.90 and 14.81- 19.75 respectively. Ratio of SiO_2/ Fe_2O_3 in laterites is less than 1.33 which indicates that the laterites of the study area are true laterites and plots in the ternary diagram (SiO_2- Fe_2O_3- Al_2O_3) indicate moderate to strong zone of lateritisation. CIA values for the laterite of the study area range between 98.88- 99.16, while slightly lower values of CIA (94.48- 98.06) is observed for the lithomarge clay samples. A cluster of laterite plots have been formed when SiO_2, Fe_2O_3, TiO_2, and CaO is plotted against CIA. The best linear correlation is observed for Na_2O and LOI. Two distinct zones of laterite and lithomarge clay are formed when CIA is plotted against Al_2O_3. The average product index (PI) of laterite is 20.80 and that of lithomarge clay is 42.56, which indicates more intense leaching of silica and other oxides in the duricrust laterite than lithomarge clay.

Keywords: Bamnoli range, Laterite, Lithomarge clay, Basalt, XRD, IR, XRF, CIA, PI.

1. Introduction

Laterite is the product of intense and prolonged chemical weathering in a hot and humid climate (Babechuk et al., 2013), wherein during the first stage of weathering most mobile elements like Mg, Ca, Na, ±K and retention of Fe, Al and Si causes mineralogical transformations (Nesbitt et al., 1980; Chesworth et al., 1981; Kronberg and Nesbitt, 1981). Work on Indian laterite especially in terms of geochemistry and mineralogical changes during lateritisation were carried out earlier by many workers (Roy Chowdhury, 1958; Roy Chowdhury et al., 1964; Sahasrabudhe and Deshmukh, 1981; Meshram and Randive, 2011; Jadhav et al., 2012). Geochemistry of major oxides and trace elements along with mineralogical study of upland laterites of Tarale- Thoseghar was helpful in ascertaining the genesis of these laterites and their relation with the underlying parent rock basalt.

Tarale- Thoseghar plateau is a part of Bamnoli range and covers a part of Satara district of Maharashtra, India (Fig. 1). The plateau runs almost in an east-west direction and becomes the drainage divide for Urmodi and Tarali streams, which are tributaries of Krishna River. The study area is bound by latitude 17°32Œ§ and 17°39Œ§ N and longitude 73°50Œ§ and 73°58Œ§ E, of SOI topographic sheet no. 47 G/14 on the scale 1:50,000. Average rainfall is 1700mm/yr, and average temperature 28°C.

2. Geology of the Study Area

Most of Maharashtra region is covered by the Deccan basaltic lava flows of tholeiitic compositions, which covers 500,000 km² areas. The Deccan basalts of Bamnoli range belong to the Wai subgroup.

Laterites capping the basaltic lava flows form plateaus and mesas at height about 1000 m AMSL, are called as "high level laterites" with an average 30 m thickness (Sahasrabudhe and Deshmukh, 1981; Widdowson and Cox, 1996; Widdowson, 1997). Laterite is reddish brown in colour with pisolitic/oolitic, vesicular, mottled, compact/massive, vermicular and brecciated structure (Fig.2a- d). Lithomarge clay / Saprolite present below the hard laterite, is reddish, yellowish red to yellow

Journal of Applied Geochemistry
Vol. 20, No. 4 (2018).pp. 432-442

PETROGRAPHICAL AND MINERALOGICAL STUDIES ON LATERITIC BAUXITE PROFILES OF SHAHUWADI TALUKA OF KOLHAPUR DISTRICT, MAHARASHTRA

[1]J. V. Khanapurkar, [2]R. A. Suryawanshi, [1]R. V. Desai, [1]S. R. Patil, [1]S. H. Patil, [1]V. R. Mali and [1]P. B. Pisal
[1] *Department of Geology, Gopal Krishna Gokhale College, Kolhapur*
[2] *Department of Geology, Y. C. College of Science, Karad, Dist. Satara*
E-mail: jayant_kh@yahoo.co.in

Abstract

This study was carriedout with an objective to filling up the lack of information on the exact mineral paragenesis during lateritic weathering of the parent rocks, the micro-environments of formation of laterites, bauxites and associated clays, and the nature of post-diagenetic processes that affect laterites and bauxites (Khanapurkar and Suryawanshi, 2014). Laterite and bauxite deposits occurring at five localities namely Dhangarwadi, Girgaon, Udgiri, Malaiwada and Manoli of Shahuwadi Taluk of Kolhapur district of Maharashtra were investigated in this study.

Petrographic examination of thin sections of bauxites, laterites and basalt from these areas show that they are composed mainly of gibbsite and cliachite, with a minor proportion of boehmite, goethite, hematite, limonite and kaolinite. Thin sections of various lithological variants from many profiles, ranging from fresh basalt to laterite, obtained from different locations, positioned to cover the entire length of the plateau, were also petrographically examined.

Keywords: Deccan Trap, Laterite, Bauxite, Petrography, Gibbsite, Cliachite.

1. Introduction

Deccan Trap basalts in Western Maharashtra, India progressively weather insitu to laterites and bauxites via an intermediate stage of saprolitic clays. The unweathered basalts are predominantly composed of a calcic plagioclase and a ferrous pyroxene, with a minor proportion of magnetite, ilmenite, volcanic glass, iddingsite and palagonite. Dissolution etch pits have formed due to weathering on the surface of minerals in these basalts (Khanapurkar and Suryawanshi, 2015).

Weathered basalts are composed of various combinations of smectites, kaolinites, goethite, hematite and anatase. Kaolinite is the principal mineral in saprolitic clays overlying the basalts in the residual bauxite deposits. It commonly forms a framework of submicron sized, irregular shaped platelets, and occasionally occurs as booklets of hexagonal platelets that rarely form spheroidal aggregates. Residual laterites overlying the saprolitic clays exhibit vesicular, spongy and pisolitic macrotextures and are composed mainly of hematite and goethite with a minor proportion of gibbsite, kaolinite and anatase (Roy Chowdhury et al, 1965; Khanapurkar and Suryawanshi, 2015). Bauxites, which occur as pockets and lenses within the laterites , display pisolitic , massive and nodular microtextures, and are predominantly composed of gibbsite with minor amounts of anatase, kaolinite , hematite and goethite. Laterites and bauxites are characterized by framework microtexture formed by three-dimensional packing of the crystallites (Chitale, 1986). The study area considered here i.e. Shahuwadi Taluk in Kolhapur District represents only Western Maharashtra, India (Fig-1.).

2. Materials and Methods

Laterites and bauxites of western Maharashtra occur as a capping over the Deccan Trap basalts covering wide regions. Laterites and bauxites of Shahuwadi Taluk represent high-level deposits occurring at elevations of over 1000m. Representative in-situ sampling of the weathered profiles was carried out at twenty locations in Shahuwadi Taluk of Kolhapur district in western Maharashtra(Fig.1.). The samples were studied megascopically and microscopically.

2.1 Sample Collection

Nineteen representative samples of laterites, bauxites, and Deccan Trap basalts were collected from the bauxite deposits in Shahuwadi region of western Maharashtra. The samples were carefully chosen in order

Journal of Structural Geology 117 (2018) 219–236

Contents lists available at ScienceDirect

Journal of Structural Geology

journal homepage: www.elsevier.com/locate/jsg

Emplacement and growth of alkaline dikes: Insights from the shonkinite dikes (Elchuru alkaline complex, SE India)

Sachin S. Ghodke, K. Rathna, Gaurav J. Kokandakar, B. Nagaraju, Laxman B. More, Munjaji V. Bhosle, K. Vijaya Kumar*

School of Earth Sciences, SRTM University, Nanded, 431606, Maharashtra, India

ARTICLE INFO

Keywords:
Alkaline magma
Dike
Shonkinite
Emplacement
Structural geology
India

ABSTRACT

The Mesoproterozoic Elchuru alkaline complex in the Prakasam Alkaline Province (PAP), Eastern Ghats Belt, SE India is intruded by coeval shonkinite dikes. Magmas parental to both the host nepheline syenite and shonkinite dikes formed during ca. 1350 Ma continental-rift related magmatism. The shonkinite dikes show fine-to medium-grained equigranular to foliated textures with clinopyroxene, biotite, amphibole, K-feldspar perthite and nepheline as major mineral phases. The dikes grew by inflation and coalescence of dike segments along intrusive steps, anastomosis and subsequent coalescence, and thermal/mechanical erosion of the host rocks. A few dikes resulted by filling the fractures created by shearing. Inflation of intrusive steps between magma segments by Mode I opening is the major mechanism of shonkinite dike emplacement and growth. However, the shonkinite dikes also demonstrate the application of remote shear stress on the dike walls resulting in anastomosis, entrapment and segmentation of tabular host rock xenoliths, and in extreme cases brecciation of the host rocks under volatile-rich and low-viscous melt conditions. Fractal analysis of xenolith-bearing dike further illustrates that thermal erosion was facilitated and accentuated by mechanical breakdown of host rock xenoliths due to interactions of tensile and shear forces. Cross-cutting relationships between the shonkinite dikes suggest local deviation in the least compressive stress direction during dike emplacement. The shonkinite dikes of Elchuru demonstrate that spatially- and temporally-restricted high-volatile low-viscous alkaline magmas may have distinctly different styles of emplacement, as controlled by interaction of near field (magmatic) tensile stress and far field (tectonic) shear stress, in an evolving continental-rift setting.

1. Introduction

Dikes offer physical evidence to understand the mechanisms of magma transportation in the Earth's crust. Emplacement and growth of dikes also provide clues to crustal evolution at scales ranging from that of a fracture to fragmentation of supercontinents. Dikes inject either through pre-existing fractures or create their own pathways by hydraulic magmatic fracturing involving the dilation of country rocks (Walker et al., 2017). Additionally, viscous indentation and fluidization of the host rock can also facilitate dike emplacement (Schofield et al., 2012a,b; Spacapan et al., 2016a). Dike emplacement occurs by hydraulic magmatic fracturing when magma pressure exceeds the lithostatic pressure. It is generally assumed that the dikes emplace perpendicular to least compressive stress σ_3 (Anderson, 1951; Gudmundsson, 1990) provided the magma propagates in self-generated hydraulic fissure. In the hydraulic magmatic fracturing model dike tips tend to be irregular to sub-rounded whereas in pre-existing fracture-fill model the dike tips would be straight and wedge-shaped (Motoki and Sichel, 2008). Examples of dikes emplacing in both self-generated (Anderson, 1938; Delaney et al., 1986) or in pre-existing (Currie and Ferguson, 1970; Baer et al., 1994; Jolly and Sanderson, 1995) fissures both exist. However, dike emplacement is not restricted to mode I (tensile) fractures alone. If the differential stress at the site of dike injection, due to addition of tectonic stress to the magma pressure, is greater than $-4T$ (where T is the tensile strength of the rock) then the rock will fail by shear stress and the dike will be injected into the shear fractures at oblique angles to the principal stresses (Escher et al., 1976; Delaney et al., 1986; Correa-Gomes et al., 2001; Khodayar and Einarsson, 2002; Paquet et al., 2007; Skarmeta, 2011; Gerbault, 2012; Spacapan et al., 2016b; Morozov et al., 2017). Dikes may also propagate and grow through thermal erosion of the country rocks in a non-dilation environment (Fialko and Rubin, 1999).

Magma pressure and the regional stress field in addition to the host rock characteristics are the dominant factors that control the length/

* Corresponding author.
E-mail address: vijay_kumar92@hotmail.com (K. Vijaya Kumar).

https://doi.org/10.1016/j.jsg.2018.09.016
Received 24 December 2017; Received in revised form 25 September 2018; Accepted 25 September 2018
Available online 29 September 2018